Available online at www.sciencedirect.com
ScienceDirect

Quaternary Research 69 (2008) 117–129

QUATERNARY RESEARCH

www.elsevier.com/locate/yqres

Numerical simulation of the paleohydrology of glacial Lake Oshkosh, eastern Wisconsin, USA

James A. Clark [a,*], Kevin M. Befus [a], Thomas S. Hooyer [b], Peter W. Stewart [a], Taylor D. Shipman [a], Chris T. Gregory [a], Deborah J. Zylstra [a]

[a] *Department of Geology and Environmental Science, Wheaton College, Wheaton, IL 60187, USA*
[b] *Wisconsin Geological and Natural History Survey, Madison, WI, USA*

Received 10 January 2007
Available online 26 November 2007

Abstract

Proglacial lakes, formed during retreat of the Laurentide ice sheet, evolved quickly as outlets became ice-free and the earth deformed through glacial isostatic adjustment. With high-resolution digital elevation models (DEMs) and GIS methods, it is possible to reconstruct the evolution of surface hydrology. When a DEM deforms through time as predicted by our model of viscoelastic earth relaxation, the entire surface hydrologic system with its lakes, outlets, shorelines and rivers also evolves without requiring assumptions of outlet position. The method is applied to proglacial Lake Oshkosh in Wisconsin (13,600 to 12,900 cal yr BP). Comparison of predicted to observed shoreline tilt indicates the ice sheet was about 400 m thick over the Great Lakes region. During ice sheet recession, each of the five outlets are predicted to uplift more than 100 m and then subside approximately 30 m. At its maximum extent, Lake Oshkosh covered 6600 km^2 with a volume of 111 km^3. Using the Hydrologic Engineering Center-River Analysis System model, flow velocities during glacial outburst floods up to 9 m/s and peak discharge of 140,000 m^3/s are predicted, which could drain 33.5 km^3 of lake water in 10 days and transport boulders up to 3 m in diameter.

Keywords: Lake Oshkosh; Outburst flood; Glacial isostasy; Paleohydrology; GIS; Great Lakes; Proglacial lake

Introduction

Studies of the proglacial and postglacial lakes of the Great Lakes region have extended over more than a century (Spencer, 1888; Goldthwait, 1908; Leverett and Taylor, 1915). Prominent in this work was the tracing of lake shorelines that are now tilted relative to the present geoid by viscous deformation of the earth's mantle subsequent to ice sheet unloading. These early studies, based upon extensive field work, described how the drainages of the lakes adjusted as lake outlets became ice-free during deglaciation and the earth experienced glacial isostatic adjustment. The first attempt to model the tilt of Great Lakes shorelines was by Gutenberg (1933) and much later by Broecker (1966), Brotchie and Silvester (1969) and Walcott (1970). The development of more realistic models of the glacial isostatic process on a spherical viscoelastic earth with realistic ice sheet loads and meltwater loading of the oceans has progressed steadily (Cathles, 1975; Clark et al., 1978; Wu and Peltier, 1983; Tushingham and Peltier, 1991; Milne et al., 1999). Although most of this work was concerned with sea level changes, some studies have focused on tilting of lake shorelines (Clark et al., 1990, 1994; Tushingham and Peltier, 1992).

Verification of the numerical predictions of these lake shorelines was difficult because predictions could not be reliably tested in the field. The availability of high resolution digital elevation models (DEMs) has contributed to this work in that, once isobases are determined from field observations of tilted shorelines, the entire region can be deformed until the shoreline is level and the ancient topography reproduced. This has been done for glacial Lake Agassiz, north of the Great Lakes (Leverington et al., 2002b), and for the Great Lakes basin (Lewis et al., 2005). Not only is shoreline tilt of interest to glacial

* Corresponding author.
E-mail address: James.A.Clark@wheaton.edu (J.A. Clark).

0033-5894/$ - see front matter © 2007 University of Washington. All rights reserved.
doi:10.1016/j.yqres.2007.10.003

geologists and geophysicists, but also the glacial outburst events common to proglacial lakes may have significantly affected climate as cold freshwater discharged rapidly into oceans (Hostetler et al., 2000; Clark et al., 2001, 2003).

Recent studies of the volume of Lake Agassiz are quickly advancing our understanding of the role of this mechanism in climate change (Leverington et al., 2002a; Teller et al., 2002). The goal of this paper is to show how Geographical Information System (GIS) methods can use numerical predictions of glacial isostatic adjustment and DEMs to predict the hydrologic evolution of proglacial lakes. The approach is demonstrated through analysis of glacial Lake Oshkosh, a proglacial lake that once occupied eastern Wisconsin.

Glacial Lake Oshkosh

Glacial Lake Oshkosh formed in front of the Green Bay Lobe of the Laurentide ice sheet in eastern Wisconsin as the ice sheet position fluctuated between 17,000 and 12,000 cal yr BP. The lake was first recognized in 1849 by Whittlesey with subsequent work extending to the present adding detail (Warren, 1876; Upham, 1903; Thwaites, 1943; Wielert, 1980a,b; Hooyer, 2007). Although there are documented readvances of the Green Bay Lobe creating numerous lake phases of glacial Lake Oshkosh (e.g., Mickelson et al., 1984), the last occurrence is well documented because it buried the Two Creeks forest bed that has been dated to about 13,600 cal yr BP. Subsequent recession of the Green Bay Lobe resulted in the opening of lower outlets and complete draining of the lake by 12,900 cal yr BP. The margin of the Green Bay Lobe at 13,600 cal yr BP is well known because it deposited a conspicuous moraine that rims the basin. It is this time period following this last readvance of the Green Bay Lobe that is the focus of the present study. Fine-grained lake sediments are ubiquitous in the lake basin but shoreline features are not well developed. Boulder lag deposits from wave-washed till are the most common indicators of water level. Initial discharge from the lake was southward through the Dekorra outlet, adjacent to and south of the Portage outlet recognized by Wielert (1980), to the lower Wisconsin River Valley. With continued recession of the Green Bay Lobe towards the northeast, a series of four, successively lower outlets opened (Fig. 1). When these northern outlets were used, glacial Lake Oshkosh discharged eastward to the Lake Michigan basin and then southward to the Gulf of Mexico (Hansel et al., 1985).

Modeling method

The method we use to reconstruct ancient hydrology uses predictions of glacial isostasy and digital elevation data as input to a geographic information system (GIS). The resulting predictions of shorelines and outburst floods are calculated solely from first principals, without the need to initially establish outlet locations, elevations or observations of shoreline tilt. We start by reviewing our method for calculating glacial isostatic effects upon shoreline tilt and then discuss how GIS methods use these predictions to reconstruct ancient lakes. Once lake extents are known we show how to estimate the magnitude and duration of the glacial outburst events that catastrophically drained the lakes.

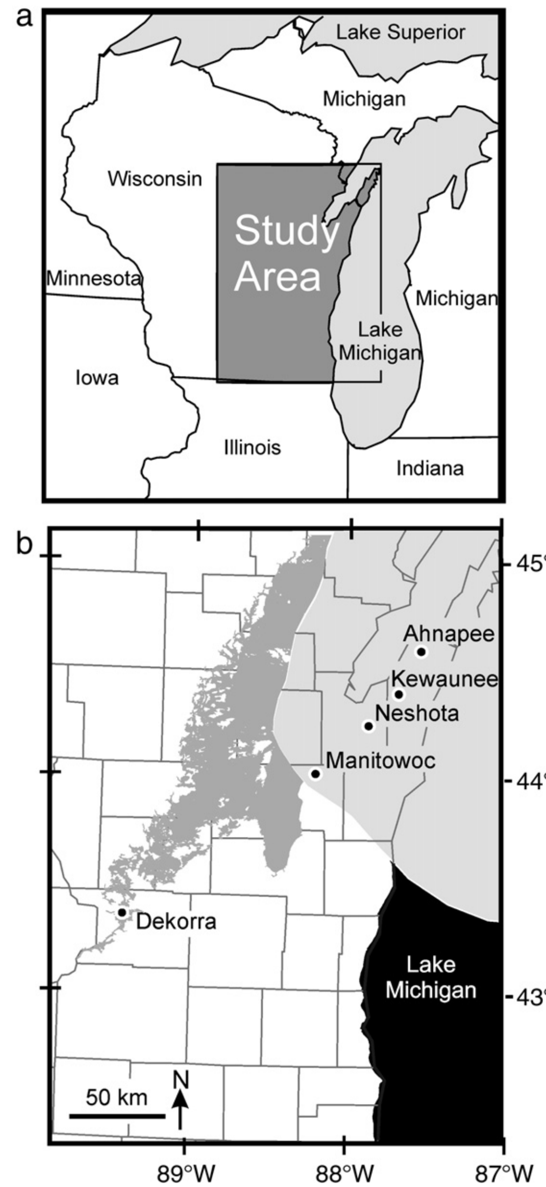

Figure 1. (a) The study area in eastern Wisconsin. (b) Glacial Lake Oshkosh, shown here at its maximum extent, formed beyond the retreating Green Bay Lobe of the Laurentide ice sheet. Five outlets controlled different phases of the lake.

Effects of earth surface loads

If the earth behaves as a linear viscoelastic radially stratified self-gravitating sphere under the influence of surface loads, then the time-dependent relative sea-level change, s, anywhere on the earth's surface resulting from ice sheet melting can be calculated (Farrell and Clark, 1976):

$$s(r,t_n)=\frac{1}{g}\left[\iint_{\text{ocean}}\rho_w s(r',t_n)G^{\mathrm{E}}(r-r')dr'+\iint_{\text{ice}}\rho_I I(r',t_n)G^{\mathrm{E}}(r-r')dr'\right.$$
$$\left.+\sum_{i=1}^{n}\iint_{\text{ocean \& ice}}L_i(r')G^{\mathrm{HV}}(r-r',t_n-t_i)dr'\right]$$
$$-K_{\mathrm{e}}(t_n)-K_{\mathrm{c}}(t_n) \quad (1)$$

https://doi.org/10.1016/j.yqres.2007.10.003 Published online by Cambridge University Press

with r and r' representing locations on the earth's surface, t_n the desired time measured from the start of the model run, and I the ice sheet thickness. L_i is the incremental load change of either ice or water load occurring at discrete 1000-yr times t_i, and in Eq. (1) there are n of these discrete times. G^{E} is the elastic Green's function giving the immediate elastic potential perturbation of the earth's geoid relative to the solid surface due to a point load of unit mass at distance $r-r'$. G^{HV} is the Heaviside Green's function describing the corresponding effect of a point mass remaining on the earth for length of time t_n-t_i (Peltier, 1974). G^{E} and G^{HV} are dependent upon the choice of viscoelastic earth structure. The constants g, ρ_w and ρ_I are the acceleration due to gravity, density of water and density of ice, respectively. The first two terms of Eq. (1) give the immediate elastic earth response to water and ice loads. The third term describes the slow viscous response resulting from all previous load changes. Finally, K_{e} and K_{c} insure the conservation of water mass as ice sheets melt and their meltwater flows into the ocean. K_{e} is the cumulative oceanwide average sea-level rise, usually called the eustatic sea-level rise, since initiation of the model run and is defined as:

$$K_{\mathrm{e}}(t_n) = \frac{\rho_I}{\rho_w A_{\mathrm{o}}} \iint_{\mathrm{ice}} I(r', t_n) dr'$$

with A_{o} the ocean area assumed here to be constant. Because oceans are irregularly distributed over the globe and because the average potential perturbation deformation of the Green's functions is non-zero, K_{c} must also be included to account for the oceanwide average earth deformation forced by the loads. This term can be calculated from:

$$\begin{aligned} K_{\mathrm{c}}(t_n) = \frac{1}{gA_{\mathrm{o}}} & \left\{ \iint_{\mathrm{ocean}} dr' \left[\iint_{\mathrm{ocean}} \rho_w s(r', t_n) G^{\mathrm{E}}(r'-r') dr' \right.\right. \\ & \left.\left. + \iint_{\mathrm{ice}} \rho_I I(r', t_n) G^{\mathrm{E}}(r'-r') dr' \right] \right\} \\ & + \frac{1}{gA_{\mathrm{o}}} \left\{ \iint_{\mathrm{ocean}} dr' \sum_{i=1}^{n} \iint_{\mathrm{ocean\&ice}} L_i(r') G^{\mathrm{HV}}(r'-r', t_n - t_i) dr' \right\} \end{aligned}$$

Eq. (1) can be solved numerically for realistic ice and ocean configurations if both the ice sheet history and earth viscoelastic structure are known. At the outset neither the sea level loadings nor the K correction terms are known but these evolve during the solution process so that eventually all are determined. Such solutions have led to increased understanding of the interactions among ice sheets, sea level and earth/geoid deformations (e.g., Clark et al., 1978, Tushingham and Peltier, 1991). Additional refinements to Eq. (1) include effects of rotational perturbations (Wu and Peltier, 1984; Milne and Mitrovica, 1996) and variation in ocean bathymetry near the shoreline causing the ocean load to transgress or regress (Clark and Bloom, 1979; Peltier, 1994). However, neither the earth viscosity structure nor the ice sheet thickness history is well known (Hughes et al., 1981; Boulton et al., 1985; Sabadini et al., 1991). During the past decade, modifications of the ice sheet history and earth structure used in models of viscous flow forced by surface (ice sheet) loads have resulted in progressively improved fit to the global Holocene sea-level data. This process of "tuning up" the models has resulted in much insight regarding the earth's ice sheets and its viscosity structure. In this study, we use the VM2 viscosity model, determined by Peltier (1996, 1999) from inversion of global relative sea level data, and the ICE-3G ice sheet thickness model (Tushingham and Peltier, 1991). Improved ice sheet models exist (i.e., ICE-4G [Peltier 1994] and ICE-5G [Peltier 2004]) but these were not reported as time-dependent thicknesses (only as elevations) and so could not be employed here. More recently the ICE-5G ice sheet thicknesses have been made available (Peltier and Fairbanks, 2006) and this chronology will be used in subsequent research.

Tilting of lake shorelines and shoreline elevations

The preceding discussion was given in the context of *sea-level* changes, which was appropriate because much of the data constraining global ice sheet thickness is derived from relative sea-level curves and because it is necessary to solve Eq. (1) to determine all surface loads, both ice and water. In this paper, we are interested in shoreline tilting of inland lakes that are not constrained to lie on the same gravitational equipotential surface as sea level but will necessarily lie on a gravitational equipotential surface parallel to sea level. Therefore, a similar approach is used to predict shoreline elevation and tilt (Clark et al., 1990). If we desire to predict a change in "sea level" at any arbitrary location, either within or beyond an ocean, we simply solve Eq. (1) at the desired location utilizing the prescribed ice loads, calculated ocean water loads and the resulting conservation of mass corrections. The *change* in elevation of a lake shoreline between two locations r and r' at time t is $s(r, t)-s(r', t)$. In the model time, t, is defined with respect to the start of the model run, 30,000 yr ago, but we measure time relative to the present, t_{p} years after the first time step of the model. To determine the change in elevation relative to present, we simply find $\Delta e(r-r', t_{\mathrm{p}}-t)=s(r, t)-s(r, t_{\mathrm{p}})-s(r', t)+s(r', t_{\mathrm{p}})$. But Δe is still unconstrained because it is only a *change* in elevation. To determine the true elevation of the shoreline at location r' at time $t_{\mathrm{p}}-t$ years ago, we need to know the present elevation of the shoreline at one point $e(r, t_{\mathrm{p}})$. The predicted lake surface must then lie on the surface defined by

$$\phi(r', t_{\mathrm{p}} - t) = e(r, t_{\mathrm{p}}) + \Delta e(r - r', t_{\mathrm{p}} - t)$$

where r' can vary over the entire region of interest. Only where this possible lake surface intersects present topography will we expect to find a shoreline from the ancient lake. It is also possible to track the time-dependent change in elevation of an outlet relative to the present elevation of the outlet, $e(r, t_{\mathrm{p}})$:

$$\begin{aligned} e(r, t_{\mathrm{p}} - t) = e(r, t_{\mathrm{p}}) + s(r, t) + K_{\mathrm{e}}(t) + K_{\mathrm{c}}(t) - s(r, t_{\mathrm{p}}) \\ - K_{\mathrm{e}}(t_{\mathrm{p}}) - K_{\mathrm{c}}(t_{\mathrm{p}}). \end{aligned}$$

Including the "K" terms is now necessary because a lake outlet is not affected by the change in volume of water in the oceans and yet these factors are included when Eq. (1) determines s. It was this procedure that Clark et al. (1994) used to determine isobases on tilted shorelines of the Great

https://doi.org/10.1016/j.yqres.2007.10.003 Published online by Cambridge University Press

Lakes. At that time it was difficult to assess the predictions because it was difficult to determine where the predicted water plane intersected the modern topographic surface. Furthermore, meltwater loading of the oceans was not included in that earlier work, whereas it is included in the present study.

GIS determination of paleo-topography

DEMs are now readily available for the Great Lakes region and allow the prediction of the exact location of a shoreline of a given age. Furthermore, it is possible to relax the requirement that the modern shoreline elevation at one point be known and to predict where shorelines should occur without prior knowledge of a known elevation somewhere on the shoreline (e.g., $e(r, t_p)$). The entire hydrologic history of a region can be determined using only the DEM and model predictions of glacial isostatic adjustment.

Using the ice and ocean loads determined from Eq. (1), we calculate deformation of the earth's surface relative to the present geoid at time $t_p - t$ years ago as

$$d(r, t_p - t) = s(r, t) + K_e(t) + K_c(t) - s(r, t_p) - K_e(t_p) - K_c(t_p)$$

on a grid of points over the region of interest. The surface is smoothly varying and can be accurately interpolated using GIS with a two-dimensional spline function to form a raster grid with the same resolution as the DEM. Subtraction of this deformation surface from the present DEM yields a "paleo-DEM" containing elevations relative to present sea level at the indicated time.

Paleohydrology predictions

With the construction of the paleo-DEM, it is possible to use GIS to calculate the ancient surface hydrology that will usually differ dramatically from present hydrology. Both ArcGIS and GRASS (Geographic Resources Analysis Support System) have extensions, Spatial Analyst/Hydro and Terraflow, respectively, that can determine drainage basins and integrated stream networks from a DEM. If there is a closed depression in the DEM, the extensions treat it as a sinkhole and allow water to drain vertically out of it as a disappearing stream. Normally a disappearing stream is not desired so there is an option to "fill the sinks." This "fill sinks" algorithm is widely used to correct for slight errors in the DEM when determining modern integrated drainage patterns. For our application, the fill sinks algorithm is critical in the determination of the location of the ancient proglacial lakes because the GIS program fills each closed depression until surface water begins to overflow. It is clear that this procedure actually defines the lake surface, because a closed depression in an integrated stream system would fill until its water level reaches an outlet elevation. Ancient lakes are thus defined by the difference between the original and the "filled" paleo-DEM. Where there is no filling of a depression the difference is zero, but where a depression has been filled the difference is the water depth of the ancient lake (paleo-bathymetry). There is no need initially to define or prescribe an outlet for the lake because the GIS procedure automatically determines the outlet at the elevation that provides the lowest course for the stream in the isostatically adjusted paleo-DEM. Of course, geomorphic and sedimentologic evidence of shorelines or spillways at the predicted locations are desirable to give confidence to the model results.

It is also necessary to include an ice sheet to the north where glacial ice would have blocked lower outlets. We use an ice sheet configuration with an arbitrarily large thickness of 10,000 m for this purpose. Unlike the ice load history, which has time-dependent changes in thickness over low-resolution, individual grid cells, this ice margin must be very detailed to accurately resemble the known deglacial history.

In practice, hundreds of lakes are identified with the above method. To find the extent of the largest lakes we use another GIS procedure to seek regions that have contiguous non-zero values. Each of these lakes is then sorted by size to isolate the largest lakes for further analysis. Once the lake extent is determined, it is possible to convert the lake raster grid to a vector polygon representation containing the lake. This polygon is the shoreline of the ancient lake which can be superimposed, in the GIS, onto a Digital Raster Graphics (DRG) image of a USGS topographic map, an aerial photograph or Digital Orthophoto Quad (DOQ). These maps can then be printed and taken into the field to verify if a shoreline exists at the predicted location. Even more effective in field verification is use of a Global Positioning System (GPS) receiver connected to a laptop GIS to indicate exact location of predicted shorelines relative to the field geologist's present position.

Outlet determination

Isostatic adjustment and changes in the position of the ice margin control the lake's outlet. Once the lake extent is determined, GIS methods can determine the location of the outlet that fixes the lake surface. GIS hydrology extensions can determine how many cells contribute water through surface runoff to every cell in the map (hydrologic "accumulation" methods). Cells that have relatively few contributing cells are expected to have a small stream, whereas if many cells contribute water to a given cell then a large stream is indicated. We use this method to locate an outlet with GIS by creating a map containing the outline of a lake enlarged by one raster cell. This map is then searched for the cell with the greatest water accumulation, indicating the largest river and hence the outlet from the lake.

Glacial outburst events

We can calculate the total volume of the proglacial lake of interest from its "paleo-bathymetry." At a later time when a lower outlet becomes ice-free, the new lake level defines a smaller volume and the difference between the lake volumes is the total amount of water discharged potentially in a torrential flood. Following O'Connor (1993) and Clayton (2000), an estimate of the discharge, velocity and water depth of such a

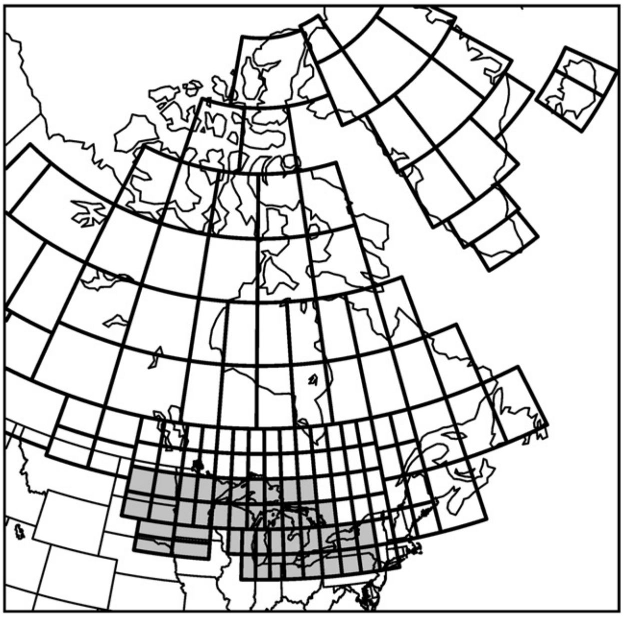

Figure 2. North American portion of the ice load grid. Grid size is reduced over the Great Lakes region. Ice thickness is constant over a given cell and varies at 1000-yr intervals. Ice thickness over the shaded portion of the grid was adjusted to be 40% of the ICE-3G thickness chronology so that predicted shoreline tilt fits field observations.

flood can be made with the Hydrologic Engineering Center-River Analysis System (HEC-RAS) model developed by the US Army Corps of Engineers Hydrologic Engineering Center (2005). HEC-RAS was designed to be a flood plain management tool that predicts stage elevation for a prescribed discharge. Input includes topographic cross sections of the river valley at representative reaches. The process of cross section construction is greatly simplified with HEC-GeoRAS, a preprocessor using a DEM and an interface to ArcGIS. HEC-RAS calculates the loss in energy between cross sections and hence the water surface profile at steady flow for subcritical, supercritical or mixed flow regimes. For our case, the roughness coefficient was assumed to be 0.04. Clayton (2000, p. 64) found the roughness coefficient to be relatively unimportant in controlling flow of Lake Wisconsin outburst events when compared to the river gradient control. The method proceeds by assigning a discharge to the highest reach in the valley resulting in a HEC-RAS prediction of stage, mean velocity, stream power and shear stress at all sections. Through subsequent assignments of varied discharges, a function relating discharge to stage height is empirically determined for a given topographic channel on the paleo-DEM at the upper portion of the channel:

$$\frac{dV}{dt} = f(\sigma) \tag{2}$$

where V is water volume and σ is stage elevation. The functional relationship, f, in this predicted rating curve strongly depends upon the topography of the channel. Because the stage of the upper reach is defined by the surface elevation of the proglacial lake, discharge through a new lower outlet can be determined immediately after the outlet becomes ice-free. Since the extent and paleo-bathymetry of the lake is known, standard GIS methods can determine the volume of the lake for any declining lake stage elevation, $\sigma = g(V)$ and so

$$\frac{dV}{dt} = f(g(V)) \tag{3}$$

with f and g empirically derived for each lake and outlet. Numerical solution of Eq. (3) yields $V(t)$ and hence the lake stage through time, $\sigma(t)$, at the highest cross section. Eq. (2) then yields discharge as the flood progressed providing the necessary input for HEC-RAS predictions of stage, velocity and transport properties of the outburst flood everywhere in the channel.

Input data

Grid of load cells

To solve Eq. (1) efficiently, the continuous ice sheet and ocean loads are approximated with a grid of cells. Upon each cell the load is assumed to be constant and the cells are bounded by latitude and longitude lines (Clark et al., 1974). Given the uncertainty in ice sheet thickness this approximation is acceptable. Furthermore, discretization in the time domain is

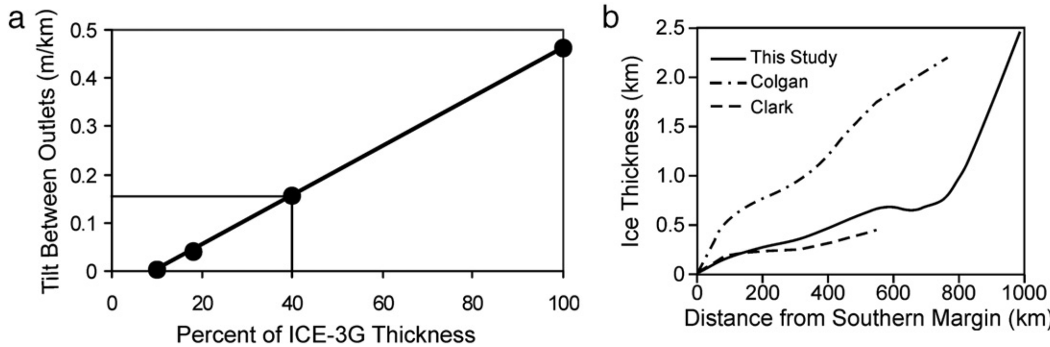

Figure 3. (a) Magnitude of shoreline tilt between the Dekorra and Manitowoc outlets between 13,600 cal yr BP and the present. When the ice thickness over the shaded region in Figure 2 is that 40% of the ICE-3G values, the model predicts the observed tilt of about 0.15 m/km. (b) Predicted ice sheet profile along a north–south transect through Lake Michigan compared to profiles suggested by Colgan (1999) and Clark (1992).

https://doi.org/10.1016/j.yqres.2007.10.003 Published online by Cambridge University Press

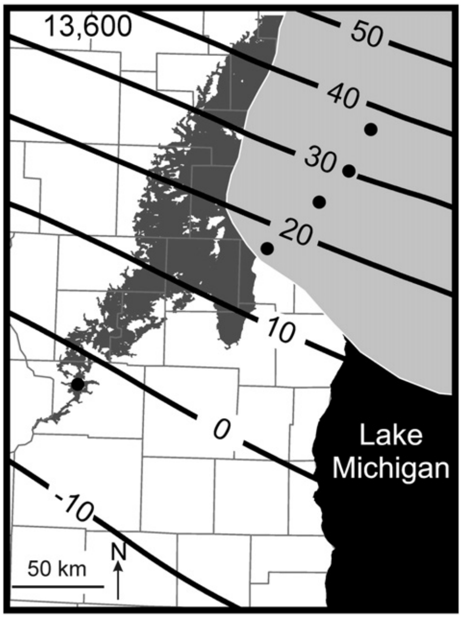

Figure 4. Predicted isobases (meters) of deformation relative to present for 13,600 cal yr BP. Shorelines of Lake Oshkosh formed at that time would now be observed tilted upwards 50 m towards the northeast between the southern and northern limits of the lake.

also required and the loads are typically assumed to change only at 1000-yr intervals with corresponding predictions of deformation at the same times. Where the ice sheet margin fluctuated quickly, spline interpolation in the time domain provides deformations and paleo-DEMs at the required times. The part of our global ice grid that is over North America is illustrated in Figure 2. Because our study is centered in the Great Lakes region the ice sheet grid has smaller resolution there than elsewhere on the global grid to represent more reliably the ice sheet over that region.

Ice-sheet history

The ICE-3G ice thickness model (Tushingham and Peltier, 1991) was used initially but that model history was based upon a radiocarbon chronology. We have therefore converted that chronology to calendar years and then interpolated to provide thicknesses at even 1000-yr intervals. Furthermore, the model assumes the ice sheet was in isostatic equilibrium at the beginning of the calculation. It is unlikely that the ice sheet was in equilibrium at its maximum extent, so we have assumed that 30,000 yr ago it was half its maximum thickness and that it thickened linearly until the glacial maximum at 22,000 cal yr BP. Upon retreat, the ICE-3G thickness chronology was used. Whereas the load history has a coarse spatial and temporal resolution, the time-dependent configuration of the ice sheet margin is critical because it is this margin that dams the proglacial lakes and therefore controls the timing of outlet occupation and lake volume. Lake history is therefore very sensitive to this margin chronology. In the model this margin approximates the ice loads but varies more dynamically than the load. The general ice margins are from Dyke (2004) but they are adjusted to provide greater detail in our specific area, and the ages of his ice margins are converted from radiocarbon to calendar years.

Digital elevation model

The digital elevation model (UTM Zone 16, NAD 83) is at 30-m spacing and provided by the Wisconsin Geological and Natural History Survey. This DEM was combined with a Lake

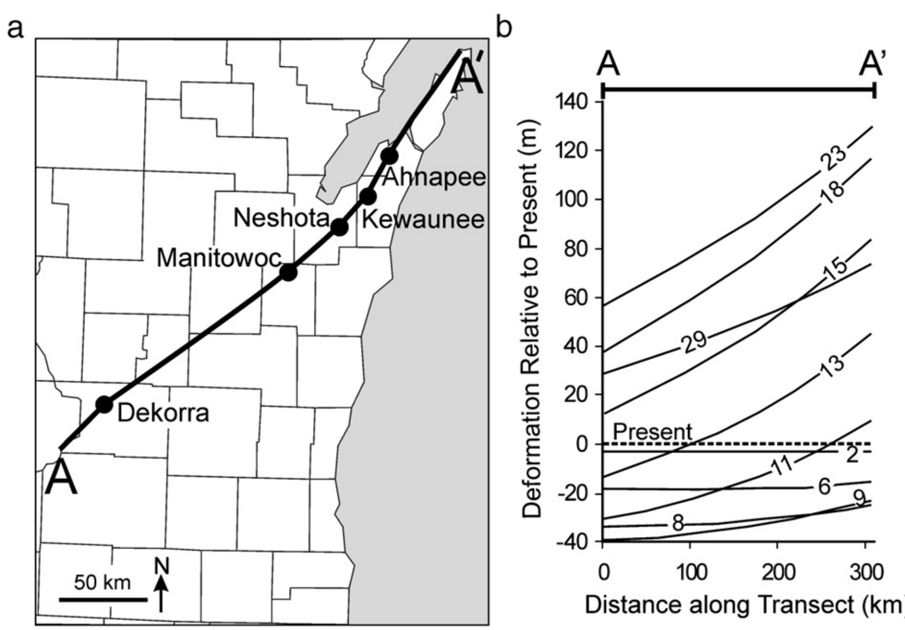

Figure 5. (a) Transect $A–A'$ through the outlets of glacial Lake Oshkosh. (b) Deformation relative to present along the $A–A'$ transect between 29,000 and 2000 cal yr BP. Curve labels are ages in 1000 cal yr BP. These deformations, when subtracted from the present DEM, give the elevations relative to present sea level. The amount of tilt and the magnitude of deformation differs at the indicated times.

https://doi.org/10.1016/j.yqres.2007.10.003 Published online by Cambridge University Press

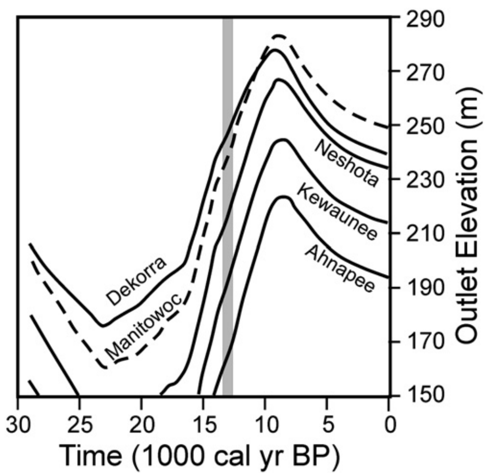

Figure 6. Time-dependent elevations of the five outlets of Lake Oshkosh. The lowest ice-free outlet controlled lake level. For our study, outlets were used between 13,600 and 12,900 cal yr BP indicated by shading. Greatest decrease in stage height occurred at 13,300 cal yr BP when levels dropped from the Manitowoc outlet to the Neshota outlet.

Michigan bathymetry data set with 100-m resolution available from the National Oceanic and Atmosphere Administration (NOAA). The DEMs were assembled at a consistent resolution of 100 m, which required resampling of the 30-m data.

Results for glacial Lake Oshkosh: application of the method

Shoreline tilt

Extensive field evidence, including geological mapping across the lake basin (Hooyer et al., 2004a,b, 2005, Hooyer and Mode, 2007), indicates that tilt between the Dekorra and Manitowoc outlets of a 13,600 cal yr BP shoreline of glacial Lake Oshkosh does not exceed 0.15 m/km. Initial tilt predictions using the ICE-3G model (Tushingham and Peltier, 1992) exceeded this value (i.e., 0.44 m/km) and so the thickness of the ice sheet over the Great Lakes region, shaded in Figure 2, was reduced by a percentage of the original ICE-3G value for all time periods. After several attempts, it was clear that the magnitude of tilt was linearly related to the thickness (Fig. 3a) and that reduction of the ice thickness over the Great Lakes to 40% of the ICE-3G amount was required. Lake Oshkosh tilt therefore suggests that the ice sheet was only about 400 m thick over the Great Lakes region. Such a thickness (Fig. 3b) is only slightly thicker than that suggested by Clark (1992) but much thinner than that proposed by Colgan (1999). Our subsequent analyses use an ICE-3G model everywhere except over the Great Lakes, where ice thickness is always 40% of the ICE-3G thickness.

Isobases and paleo-DEM

Predicted isobases for 13,600 cal yr BP (Fig. 4) indicate that tilting of a shoreline formed at that time will be upward towards the northeast, as much as 50 m relative to the Dekorra outlet. Interpolation between the isobases results in a deformation surface, which, when subtracted from the present DEM, results in a paleo-DEM over eastern Wisconsin. This surface is dynamic; Figure 5 shows deformation through time along a transect through the succession of outlets. Time-dependent elevations of Lake Oshkosh outlets (Fig. 6) also display the dynamic nature of the region. These are obtained from a time slice at fixed horizontal distances in Figure 5b. As the ice sheet advances between 30,000 and 23,000 cal yr BP the earth subsides. During ice sheet retreat uplift occurs, but approximately 9000 cal yr BP, a migrating and collapsing forebulge causes renewed subsidence which continues until the present. Late glacial and postglacial lakes forming in the Great Lakes region are therefore expected to be affected by both uplift and subsidence.

The lowest ice-free outlet controlled the associated lake level. Although the Manitowoc outlet is now higher than the Dekorra outlet, it was lower than that outlet until 11,000 cal yr BP. The present study focuses only upon the time period from 13,600 to 12,900 cal yr BP during the waning phases of glacial Lake Oshkosh (shaded area, Fig. 6). Table 1 lists predicted present outlet elevations and predicted elevations at the time each was used. All outlets were rising when they controlled lake levels and would continue to rise an additional 40 m to 60 m before subsequent subsidence reduced their elevations to

Table 1
Geometry of the five phases of Lake Oshkosh

Lake outlet	Time (cal yr BP)	Predicted outlet elevation (m)		Lake area (km^2)	Mean depth (m)	Maximum depth (m)	Lake volume (km^3)	Volume difference (km^3)	Present outlet elevation observed by others (m)		
		Present	Past						Thwaites and Bertrand (1957)	Wielert (1980a,b)	Hooyer et al. (2004a,b)
Dekorra	13,600	239.2	241.7	6624	16.9	55.5	111.7		244 (Portage)	238 (Portage)	242
Manitowoc	13,300	248.9	235.2	5553	12.7	74.6	70.4	41.4	247	248	249
Neshota	13,200	234.4	216.2	1778	20.7	64.7	36.9	33.5	233	236	233
Kewaunee	13,100	213.9	190.1	497	16.1	65.8	8.0	28.9	208	209	209
Ahnapee	12,900	193.8	167.0	1464	14.9	47.1	21.8	−13.8	195	194	194

Areas and volumes are for the ice sheet configurations of Figure 9. Other ice sheet configurations would yield different results. As an example, the ice margin is well north of the Ahnapee outlet at 12,900 cal yr BP so that lake is much larger in area and volume than the lake formed when the Kewaunee outlet was just in use. The Ahnapee phase is therefore larger than the Kewaunee phase in the table.

https://doi.org/10.1016/j.yqres.2007.10.003 Published online by Cambridge University Press

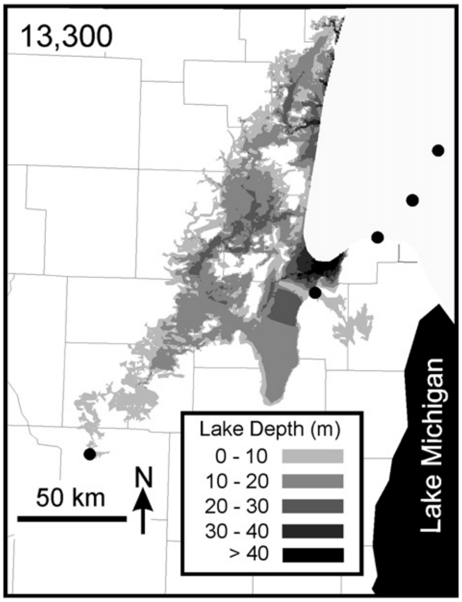

Figure 7. Predicted lake depth at 13,300 cal yr BP. Manitowoc outlet controlled the lake level.

present levels. In the case of the Dekorra outlet, this subsidence actually brought present levels below its elevation at 13,600 cal yr BP. Also included in Table 1 are observations of present outlet elevations reported in the literature (Thwaites and Bertrand, 1957; Wielert, 1980a,b; Hooyer et al., 2004a,b).

Our predicted present elevations were those elevations on the present DEM that correspond with outlet locations determined on the paleo-DEM with the GIS methods described above. The close agreement of predicted present elevations to observations lends credence to the outlet prediction method. Only for the case of the Kewaunee outlet do the predictions differ significantly from observations. That outlet had a complex history where successively lower channels, with elevations ranging from 232 m to 208 m, opened as the ice sheet retreated northward over a 5-km distance. The ice margin used in our model barely covered the lowest of these channels and so the next higher channel was predicted to control lake level.

Prediction of the lakes

Lake Oshkosh paleo-bathymetry for 13,300 cal yr BP, predicted by subtraction of the filled paleo-DEM from the paleo-DEM (Fig. 7), is used to determine volume and configuration of the lake as it drained, lowering its stage elevation. The predicted lake drained through the Manitowoc outlet and had an average depth of 12.7 m and a volume of 70.4 km^3 (Table 1). Other predicted lakes in the region were smaller but may also be helpful in assessing tilt of the region. The predicted shoreline for Lake Oshkosh is shown superimposed upon an aerial photograph, a topographic map and a shaded relief map (Fig. 8) that were helpful in field verification. Of even greater use in the field were ArcGIS shapefiles displayed on a laptop computer with a GPS locator superimposed so that quick and accurate field assessment of shorelines was possible. The entire hydrologic history of the Lake Oshkosh basin can be predicted in a similar manner and Figure 9 shows the evolution of these lakes from 13,600 to 12,900 cal yr BP. Although the ice margin at 13,600 cal yr BP (post-Two Creeks maximum) formed a prominent moraine across the lake basin, the position of the receding ice margins as lower outlets opened is not well known at this time. However,

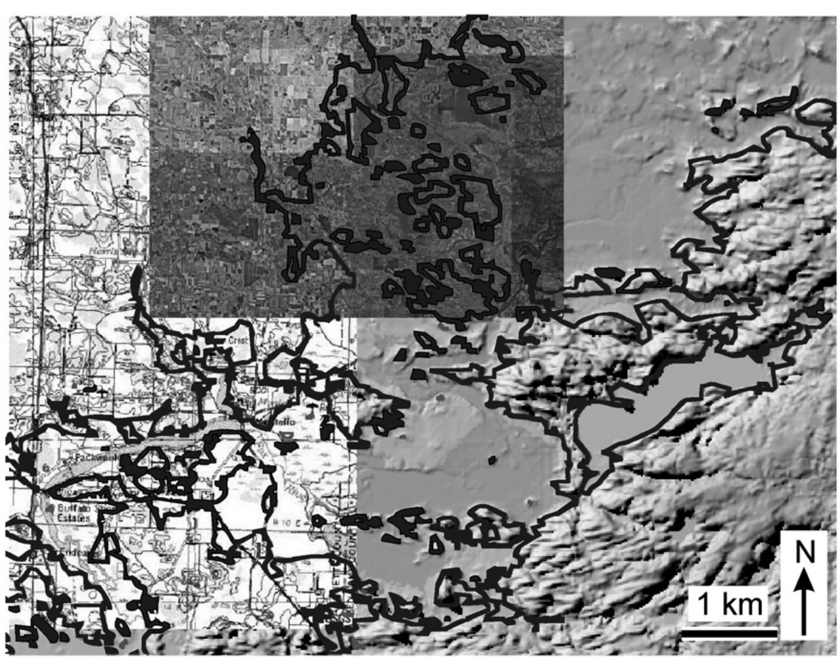

Figure 8. Example of a predicted Lake Oshkosh shoreline superimposed upon a USGS topographic map, an aerial photograph and a shaded relief map. These were used for verification of predictions in the field.

recent geological mapping in the northern part of the lake basin indicates recessional moraine segments that mimic the orientation of the ice margin at 13,600 cal yr BP. Thus, it is reasonable to assume that the ice margin receded evenly across the northern part of the lake basin.

Outburst floods

When the ice sheet receded northward from the Manitowoc outlet with an elevation of 235.3 m and uncovered the Neshota outlet at the much lower elevation of 216.2 m, much of Lake Oshkosh drained catastrophically, rapidly carving a deep channel now occupied by a very small stream (Fig. 10). However, to determine the total volume of water involved in the flood, it is necessary to know the precise ice sheet configuration in the basin at the time of the flood. If much of the basin had been ice-filled upon activation of the outlet, relatively little water would drain from the basin. Alternatively, if most of the basin was ice-free when the ice dam burst the water volume could be enormous. Because the exact ice sheet configuration is unknown at 13,200 cal yr BP, we use the likely configuration depicted in Figure 9b. When the stage drops from 235.2 m to 216.2 m, lake volume decreases from 70.4 km^3 to 36.9 km^3, providing 33.5 km^3 of water for the flood.

Assuming erosion of the channel to its modern configuration occurred very early in the event (i.e., paleo-DEM reflects present topography), the empirical relationships relating lake volume to stage elevation as determined by GIS (Fig. 11a) and HEC-RAS predictions of stage to discharge (Fig. 11a) result in a prediction of 140,000 m^3/s (0.14 Sv) maximum discharge. This

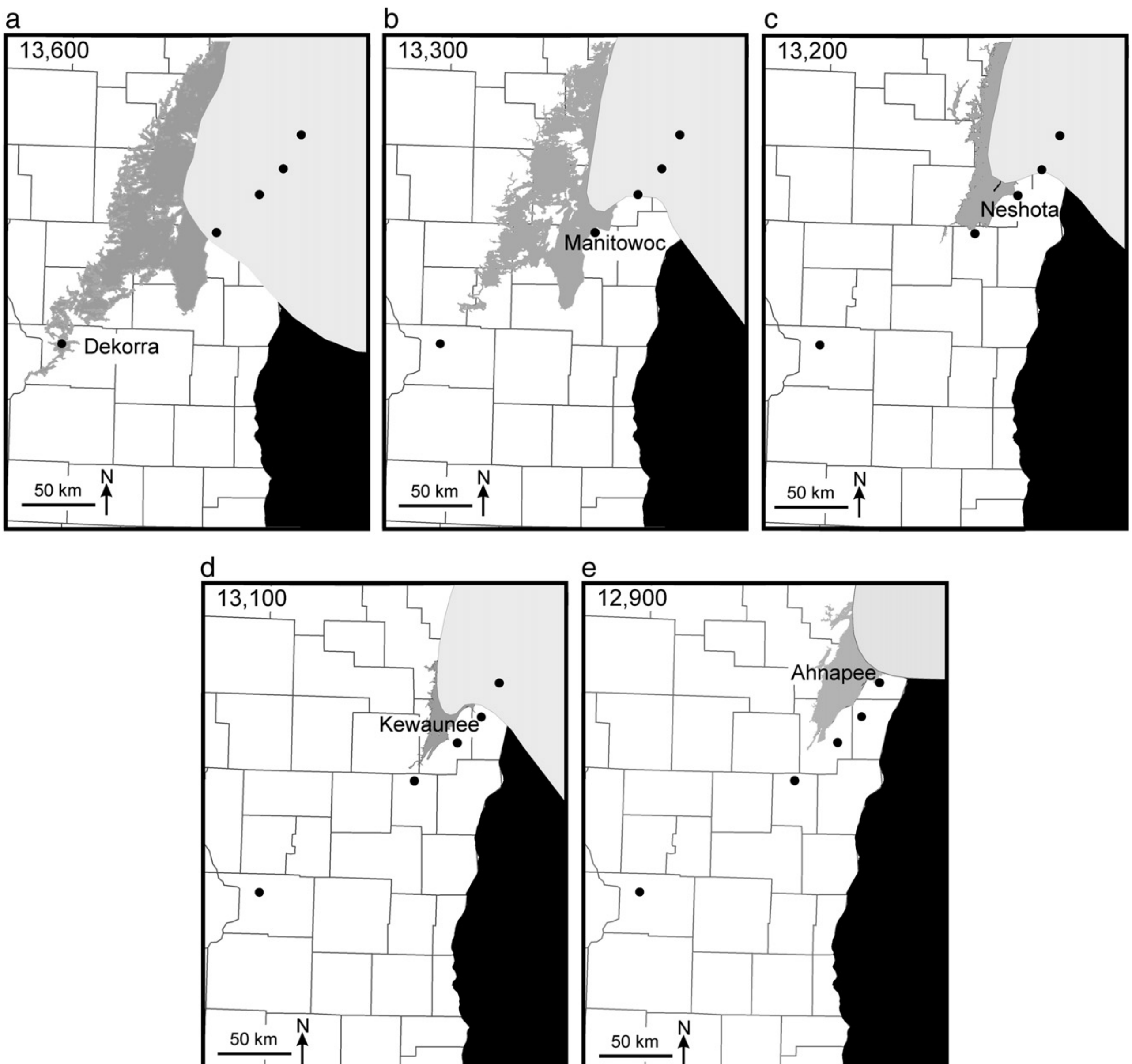

Figure 9. (a–e) Predicted lake extent at 13,600, 13,300, 13,200, 13,100 and 12,900 cal yr BP. Controlling outlets are labeled on each map.

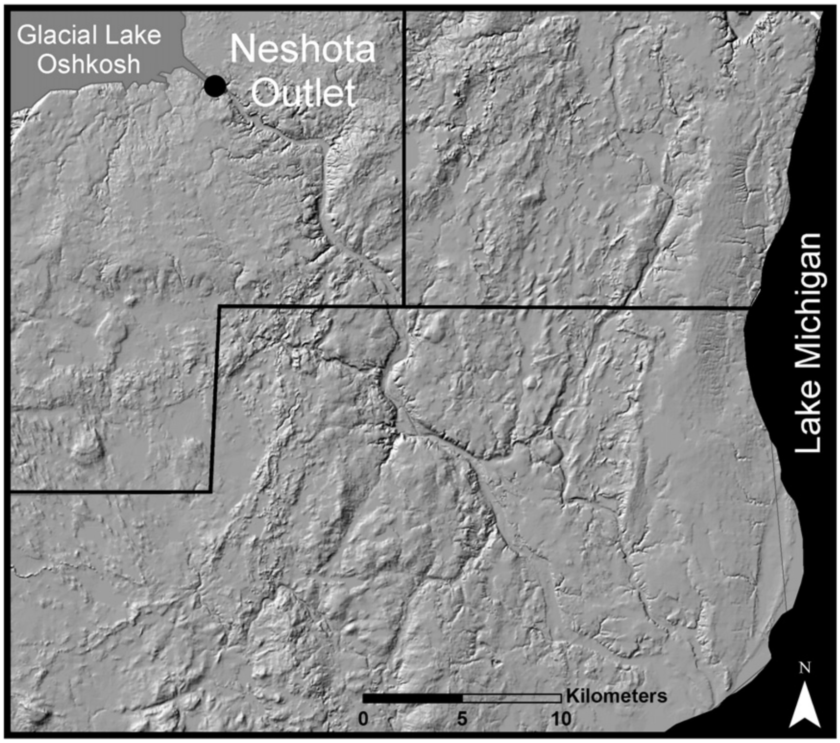

Figure 10. Shaded relief map of the Neshota outlet channel. The present stream occupying this valley is very small.

estimate assumes the outlet was instantaneously ice-free and so is undoubtedly an overestimate. Nevertheless, the flow must have been considerably larger than the peak flow of the Mississippi River during its 1993 peak flood event (43,000 m^3/s) and is comparable to that observed during the 1986 outburst event at Russell Fiord, Alaska (110,000 m^3/s; Mayo, 1989), which involved an ice-dammed lake of much less volume (5.41 km^3) than Lake Oshkosh. This Oshkosh flood was of the same magnitude for a short period as the long-term Mississippi River flow to the Gulf of Mexico (0.092 Sv) between 13,680 and 13,000 cal yr BP (Licciardi et al., 1999). Numerical solution of Eq. (2) indicates that the lake drained to the lower stage of the Neshota outlet in approximately 10 days once that outlet became ice-free (Fig. 11b). Variation of velocity and water depth with distance down the channel predicted by HEC-RAS is given in Figure 12. Relationships between stream power and shear stress to competence of a river (summarized by O'Connor, 1993, p. 57) suggest that boulders up to 3 m in diameter could be transported in the 9 m/s peak flow with shear stress of 300 to 600 N/m^2 and stream power of 1000 to 5500 watts/m^2. Boulders in a gravel pit in the Neshota channel are 2 m in size. Rounding and imbricate layering of the coarse load suggests these were transported in a flood event. Deposition of the very coarse load would occur in the channel wherever the velocity, shear stress, and stream power are low. Similar outburst floods occurred as the ice continued to recede north of the Kewaunee outlet, though the water volume affected was slightly smaller.

Discussion

The methods demonstrated here can be used throughout the Great Lakes region to predict lake extent and volume, outlet

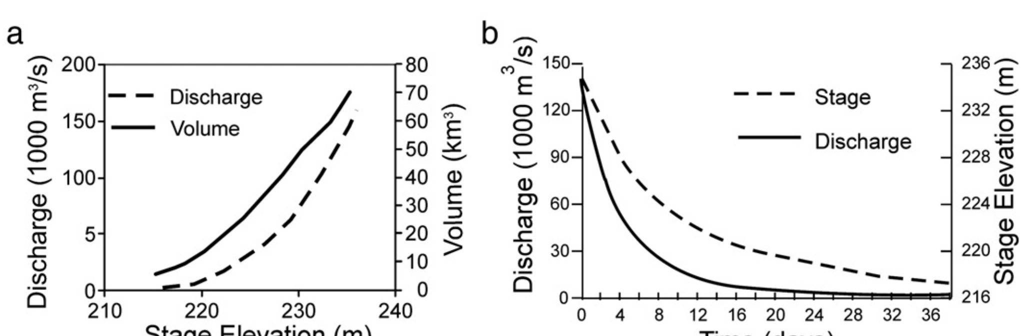

Figure 11. (a) Empirical relationship between lake volume, discharge and stage elevation for the paleo-DEM at 13,300 cal yr BP as predicted by the HEC-RAS model for the Neshota outlet and channel. (b) Time-dependent change in discharge and stage elevation from numerical solution of Eq. (2).

https://doi.org/10.1016/j.yqres.2007.10.003 Published online by Cambridge University Press

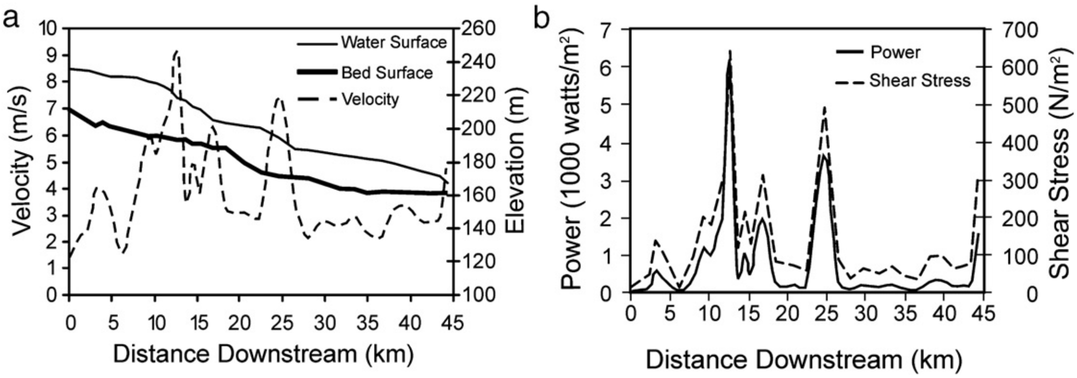

Figure 12. (a) HEC-RAS predictions for water-surface elevation and water velocity when the Neshota outlet first becomes active at 13,300 cal yr BP. Distances are measured downstream from the Neshota outlet. Bed-surface elevation is defined by the paleo-DEM. (b) HEC-RAS predictions for shear stress along the bed and stream power. Values exceeding 150 N/m^2 shear stress or 2000 $watts/m^2$ are capable of transporting boulders at least 2 m in diameter.

locations and outburst flood magnitudes as the basin evolved. As implemented here, the method only provides a lake level that would form when incipient flow commences at an outlet. This assumption is certainly incorrect because precipitation or meltwater flowing out of the outlet was likely enormous, raising the dynamic level of the lake above the sill of the outlet. For example, Hansel and Mickelson (1988) suggest glacial Lake Chicago stood 15 m above the Chicago outlet floor and that the 6-m variation in lake heights between the Glenwood and Calumet phase could be due to discharge fluctuations, not erosion at the outlet as postulated earlier (Bretz, 1951). Our predicted shorelines are therefore a minimum for lake elevation, and resulting outburst floods would be even greater than we predict.

The ICE-5G ice thickness values over the Great Lakes are similar to the ICE-3G values and therefore are almost twice the thickness we used to predict the tilting of Lake Oshkosh shorelines. The ICE-3G chronology seems to explain adequately the modern tilt rate determined from lake gauge records (Tushingham, 1992; Mainville and Craymer, 2005). The discrepancy between the ice chronology over the Great Lakes required to explain the ancient shorelines of eastern Wisconsin and the chronology needed to fit modern rates of deleveling are unresolved. Subsequent work will use geophysical inversion theory to find an ice sheet history for the region that best fits shoreline tilt and lake gauge data.

As the ice sheet retreated, much of the Great Lakes region that was once loaded with ice became flooded with lake water. This freshwater load would influence the isostatic adjustment process of the region, so a complete analysis should include this effect. Preliminary work suggests, however, that these freshwater loads contributed very little to the isostatic adjustment process, resulting in earth deformation less than 10% of the deformation forced by ice loads (Clark et al., 2007).

The hydrology GIS extensions can determine river systems and watersheds as well as lakes. It will therefore be possible to test whether glacial isostatic adjustment in the region affected surface drainage and flood magnitudes (Brooks et al., 2005). Predicted river courses in the past can be compared to present river channels with any differences likely associated with the isostatic adjustment process. Also, the groundwater flow in the region must have been greatly affected by the huge hydrostatic head under the ice sheet, the rapid and large changes in lake levels and the tilt of the landscape (Lemieux, 2006). To understand the total paleohydrology of the region, these processes will need to be included.

Now only a very small stream exists in the deeply incised Neshota valley so most of the erosion undoubtedly occurred during the outburst event. Rapid erosion of outlets and flood valleys was certainly significant, and detailed field observations of shorelines, parallel to predictions but higher in elevation, would indicate an outlet that was once higher but affected by subsequent erosion or changes in discharge. Similarly, the relationship of stage to discharge undoubtedly changed as erosion quickly occurred during flood events. Sedimentation also modified the lake bathymetry, and water volumes reported here would therefore be underestimates. Drilling in the basin indicates up to 100 m of sediment was deposited in Lake Oshkosh, but most of it occurred during lake phases prior to those in this study.

The glacial outburst flood is estimated to have a discharge capable of transporting boulders up to 3 m in diameter and the model can predict where along the channel these boulders would be deposited. The outburst event for this relatively small transition from the Manitowoc to Neshota lake phases was nevertheless capable of providing in 10 days approximately 33.5 km^3 of cold freshwater to the Gulf of Mexico at 13,300 cal yr BP. The impact of this contribution upon ocean circulation and climate is difficult to assess, especially since there were undoubtedly many similar flood events that occurred during the lifetime of glacial Lake Oshkosh, as well as other lakes that quickly drained throughout the Great Lakes basin (Lewis and Teller, 2006).

Conclusion

It is possible to predict the surface hydrologic history of any region given an ice sheet thickness model, a known earth viscoelastic structure, and a present DEM. Using these methods, reconstructions of extent and volume of glacial Lake Oshkosh in eastern Wisconsin are plausible and can be used to guide future field work in the region. The locations of outlets and their

https://doi.org/10.1016/j.yqres.2007.10.003 Published online by Cambridge University Press

relative elevations through time can also be predicted. These predicted outlets and lake geometries can be used to calculate the magnitude and duration of the Lake Oshkosh outburst floods. Evidence from transport of very large boulders, deeply incised spillways and underfit streams provide support for the predictions of these flood magnitudes. These same techniques can be used to predict lake histories and outburst flood events over a much larger region of the Great Lakes (Clark et al., 2007).

Acknowledgments

We gratefully acknowledge support from the National Science Foundation (NSF Grant EAR-0414012 and EAR-0624199), the National Aeronautical and Space Administration (NASA Grant NAG5-10348), Wheaton College, the Wheaton College Alumni Association, and the United States Geological Survey National Cooperative Geologic Mapping Program. Laura Toma provided timely help with implementation of the TerraFlow extension to GRASS. Matt Andresen, Lori McGuire and Tanya Lubansky provided assistance during the early phases of this work. The reviews of C.F.M. Lewis and Grahame Larson greatly improved the manuscript.

References

Boulton, G.S., Smith, G.D., Jones, A.S., Newsome, J., 1985. Glacial geology and glaciology of the last mid-latitude ice sheets. Geological Society of London Journal 142, 447–474.

Bretz, J.H., 1951. The stages of Lake Chicago: Their causes and correlations. American Journal of Science 249, 401–429.

Broecker, W.S., 1966. Glacial rebound and the deformation of the shorelines of proglacial lakes. Journal of Geophysical Research 71, 4777–4783.

Brooks, G.R., Thorleifson, L.H., Lewis, C.F.M., 2005. Influence of loss of gradient from postglacial uplift on Red River flood hazard, Manitoba, Canada. Holocene 15, 347–352.

Brotchie, J., Silvester, R., 1969. On crustal flexure. Journal of Geophysical Research 74, 5240–5252.

Cathles, L.M., 1975. The viscosity of the Earth's mantle. Princeton University Press, Princeton, NJ. 390 pages.

Clark, J.A., Bloom, A.L., 1979. Hydro-isostasy and Holocene emergence of South America. In: Sugio, K., Fairchild, T.R., Martin, L., Flexor, J.-M. (Eds.), Proceedings of the 1978 International Symposium on Coastal Evolution in the Quaternary. Sao Paulo, Brazil, pp. 41–60.

Clark, J.A., Farrell, W.E., Peltier, W.R., 1978. Global changes in post-glacial sealevel: A numerical calculation. Quaternary Research 9, 265–287.

Clark, J.A., Timmermans, H.M., Thomas, J., Calvin, H.S., Kenneth, J., 1994. Glacial isostatic deformation of the Great Lakes region. Geological Society of America Bulletin 106, 19–31.

Clark, J.A., Pranger, H.S., Walsh, J.K., Primus, J.A., 1990. A numerical model of glacial isostasy in the Lake Michigan basin. In: Schneider, A.F., Fraser, G.S. (Eds.), Late Quaternary history of the Lake Michigan basin. Geological Society of America Special Paper 251. Boulder, Colorado, pp. 111–123.

Clark, J.A., Zylstra, D.J., Befus, K.M., 2007. Effects of Great Lakes water loading upon glacial isostatic adjustment and lake history. Journal of Great Lakes Research 33, 627–641.

Clark, P.U., 1992. Surface form of the southern Laurentide ice sheet and its implications to ice-sheet dynamics. Geological Society of America Bulletin 104, 595–605.

Clark, P.U., Marshall, S.J., Clarke, G.K.C., Hostetler, S.W., Licciardi, J.M., Teller, J.T., 2001. Freshwater forcing of abrupt climate change during the last glaciation. Science 293, 283–287.

Clarke, G., Leverington, D., Teller, J., Dyke, A., 2003. Superlakes, megafloods, and abrupt climate change. Science 301, 922–923.

Clayton, J.A., 2000. Drainage of glacial Lake Wisconsin: Reconstruction of a Late Pleistocene catastrophic flooding episode, unpublished M.Sc. thesis, University of Wisconsin, Madison, 138 pages.

Colgan, P.M., 1999. Reconstruction of the Green Bay Lobe, Wisconsin, United States, from 26,000 to 13,000 radiocarbon years B.P. In: Mickelson, D.M., Attig, J.W. (Eds.), Glacial Processes Past and Present. Boulder, Colorado, Geological Society of America Special Paper 337, pp. 137–150.

Dyke, A.S., 2004. An outline of North American deglaciation with emphasis on central and northern Canada. In: Ehlers, J., Gibbard, P.L. (Eds.), Quaternary glaciations—Extent and chronology: Part II. Developments in Quaternary Science, vol. 2b. Elsevier, Amsterdam, pp. 373–424.

Farrell, W.E., Clark, J.A., 1976. On postglacial sea level. Geophysical Journal of the Royal Astronomical Society 46, 647–667.

Goldthwait, J.W., 1908. A reconstruction of water planes of the extinct glacial lakes in the Lake Michigan basin. Journal of Geology 16, 459–476.

Gutenberg, B., 1933. Tilting due to glacial melting. Journal of Geology 41, 449–467.

Hansel, A.K., Mickelson, D.M., Schneider, A.F., Larsen, C.E., 1985. Late Wisconsinan and Holocene history of the Lake Michigan basin. In: Karrow, P.F., Calkin, P.E. (Eds.), Quaternary Evolution of the Great Lakes, Geological Association of Canada Special Paper 30, pp. 39–53.

Hansel, A.K., Mickelson, D.M., 1988. A reevaluation of the timing and causes of high lake phases in the Lake Michigan basin. Quaternary Research 29, 113–128.

Hughes, T., Denton, G.H., Anderson, B.G., Schilling, D.H., Fastook, J.L., Lingle, C.S., 1981. The last great ice sheet: A global view. In: Denton, G.H., Hughes, T.J. (Eds.), The last great ice sheets. John Wiley and Sons, New York, pp. 263–317.

Hooyer, T.S., editor, 2007. Late-Glacial History of East-Central Wisconsin: Guide Book for the 53rd Midwest Friends of the Pleistocene Field Conference, May 18–20, 2007. Wisconsin Geological and Natural History Survey Open File Report 2007-01, 94 pages.

Hooyer, T. S. and Mode, W.N., 2007. Preliminary Quaternary geologic map of the northern fox river Lowland, Wisconsin. Wisconsin Geological and Natural History Survey Open-File Report 2007-05, 1 plate (scale 1:100,000).

Hooyer, T.S., Attig, J.W., and Clayton, Lee, 2004a. Preliminary Pleistocene geologic map of the central Fox River lowland, Wisconsin: Wisconsin Geological and Natural History Survey Open-File Report 2004-04, 1 plate (scale 1:100,000).

Hooyer, T.S., Schoephoester, P., Mode, W.N., Clayton, L., Attig, J.W., 2004b. Glacial outburst floods from proglacial lakes in Wisconsin: Geological Society of America Abstracts with Programs (Annual meeting, Denver, CO), vol. 36 n. 5, p. 281.

Hooyer, T.S., Mode, W.N., Clayton, Lee, and Attig, J.W., 2005, Preliminary Pleistocene geologic map of the southern Fox River lowland, Wisconsin: Wisconsin Geological and Natural History Survey Open-File Report 2005-03, 1 plate (scale 1:100,000).

Hostetler, S.W., Bartlein, P.J., Clark, P.U., Small, E.E., Solomon, A.M., 2000. Simulated influences of Lake Agassiz on the climate of central North America 11,000 years ago. Nature 405, 334–337.

Lemieux, J.-M. 2006. Impact of the Wisconsinian Glaciation on Canadian Continental Groundwater Flow. Ph.D. Thesis, University of Waterloo, 201 p.

Leverett, F., Taylor, F.B., 1915. The Pleistocene of Indiana and Michigan and the History of the Great Lakes. U. S. Geological Survey Monograph 53, 529.

Leverington, D.W., Mann, J.D., Teller, J., 2002a. Changes in the bathymetry and volume of glacial Lake Agassiz between 9200 and 7700 14c yr B.P. Quaternary Research 57, 244–252.

Lewis, C.F.M., Blasco, S.M., Gareau, P.L., 2005. Glacial isostatic adjustment of the Laurentian Great Lakes basin: Using the empirical record of strandline deformation for reconstruction of early Holocene paleo-lakes and discovery of a hydrologically closed phase. Géographie physique et Quaternaire 59, 187–210.

Leverington, D.W., Teller, J., Mann, T., 2002b. A GIS method for reconstruction of late Quaternary landscapes from isobase data and modern topography. Computers & Geosciences 28, 631–639.

Lewis, C.F.M., Teller, J.T., 2006. Glacial runoff from North America and its possible impact on oceans and climate. Chapter 28. In: Knight, P.G. (Ed.), Glacier Science and Environmental change. Blackwell Publishing Ltd, Oxford, UK, pp. 138–150.

Licciardi, J.M., Teller, J.T., Clark, P.U., 1999. Freshwater routing by the Laurentide ice sheet during the last deglaciation. In: Clark, P.U., Webb, R.S., Keigwin, L.D. (Eds.), Mechanisms of global climate change at millennial time scales. Geophysical Monograph 112. American Geophysical Union, Washington DC, pp. 177–201.

Mainville, A., Craymer, M.R., 2005. Present-day tilting of the Great Lakes region based on water level gauges. Bulletin of the Geological Society of America 117, 1070–1080.

Mayo, L.R., 1989. Advance of Hubbard glacier and 1986 outburst of Russell Fiord, Alaska, U.S.A. Annals of Glaciology 13, 189–194.

Mickelson, D.M., Clayton, L., Baker, R.W., Mode, W.N., Schneider, A.F., 1984. Pleistocene stratigraphic units of Wisconsin: Wisconsin Geological and Natural History Survey, Miscellaneous Paper 84-1. 499 p.

Milne, G.A., Mitrovica, J.X., 1996. Postglacial sea-level change on a rotating Earth: First results from a gravitationally self-consistent sea level equation. Geophysical Journal International 126, F13–F20.

Milne, G.A., Mitrovica, J.X., Davis, J.L., 1999. Near-field hydro-isostasy: The implementation of a revised sea-level equation. Geophysical Journal International 139, 464–482.

O'Connor, J.E., 1993. Hydrology, hydraulics and geomorphology of the Bonneville flood. Geological Society of America Special Paper 274 83 pages.

Peltier, W.R., 1974. The impulse response of a Maxwell earth. Reviews of Geophysics and Space Physics 12, 649–669.

Peltier, W.R., 1994. Ice Age paleotopography. Science 265, 195–201.

Peltier, W.R., 1996. Mantle viscosity and Ice-age ice sheet topography. Science 273, 1359–1364.

Peltier, W.R., 1999. Global sea level rise and glacial isostatic adjustment. Global and Planetary Change 20, 93–123.

Peltier, W.R., 2004. Global glacial isostasy and the surface of the ice-age earth: The ICE-5G (VM2) model and GRACE. Annual Reviews of Earth and Planetary Sciences 32, 111–149.

Peltier, W.R., Fairbanks, R.G., 2006. Global glacial ice volume and Last Glacial Maximum duration from an extended Barbados sea level record. Quaternary Science Reviews 25, 3322–3337.

Sabadini, R., Lambeck, K., Boschi, E. (Eds.), 1991. Glacial isostasy, sea-level and mantle rheology. Kluwer Academic Publishers, Boston. 708 pages.

Spencer, J.W., 1888. Notes of the origin and history of the Great Lakes of North America. American Association for the Advancement of Science, Proceedings, vol. 37, pp. 197–199.

Teller, J.T., Leverington, D.W., Mann, J.D., 2002. Freshwater outbursts to the oceans from glacial Lake Agassiz and their role in climate change during the last deglaciation. Quaternary Science Reviews 21, 879–887.

Thwaites, F.T., 1943. Pleistocene of part of northeastern Wisconsin. Geological Society of America Bulletin 54, 87–144.

Thwaites, F.T., Bertrand, K., 1957. Pleistocene geology of the Door Peninsula, Wisconsin. Geological Society of America Bulletin 68, 831–880.

Tushingham, A.M., 1992. Postglacial uplift predictions and historical water levels of the Great Lakes. Journal of Great Lakes Research 18, 440–455.

Tushingham, A.M., Peltier, W.R., 1991. ICE-3G: A new global model of Late Pleistocene deglaciation based upon geophysical predictions of post-glacial relative sea-level change. Journal of Geophysical Research 96, 4497–4523.

Tushingham, A.M., Peltier, W.R., 1992. Validation of the ICE-3G model of Wurm-Wisconsin deglaciation using a global database of relative sea level histories. Journal of Geophysical Research 97, 3285–3304.

Upham, W., 1903. Glacial Lake Jean Nicolet. The American Geologist 32, 330–331.

US Army Corps of Engineers, 2005. HEC-RAS River Analysis System, Version 3.1.3. Hydrologic Engineering Center, Davis, CA.

Walcott, R.I., 1970. Isostatic response to loading of the crust in Canada. Canadian Journal of Earth Sciences 7, 716–727.

Warren, G.K., 1876. Report on the transportation route along the Wisconsin and fox Rivers. U.S. Engineers, Washington.

Whittlesey, C., 1849. Geological report on that portion of Wisconsin bordering on the south shore of Lake Superior. In: Owen, D.D. (Ed.), Report of a Geological survey on Wisconsin, Iowa, and Minnesota, 1852. Lippincott, Grambo and Co., pp. 425–480.

Wielert, J.S., 1980a. The late Wisconsinian glacial lakes of the Fox River watershed, Wisconsin, Iowa and Minnesota. M.S. thesis, University of Wisconsin, Superior, 42 p.

Wielert, J.S., 1980b. The late Wisconsinan glacial lakes of the Fox River watershed, Wisconsin: Transactions of the Wisconsin Academy of Sciences. Arts and Letters 68, 201.

Wu, P., Peltier, W.R., 1983. Glacial isostatic adjustment and the free air gravity anomaly as a constraint on deep mantle viscosity. Geophysical Journal of the Royal Astronomical Society 74, 377–450.

Wu, P., Peltier, W.R., 1984. Pleistocene deglaciation and the Earth's rotation: A new analysis. Geophysical Journal of the Royal Astronomical Society 76, 202–242.